Fast-folding experiments and the topography of protein folding energy landscapes

PG Wolynes[1], Z Luthey-Schulten[1] and JN Onuchic[2]

The rapid folding of certain proteins can be described theoretically using an energy landscape in the shape of a folding funnel. New techniques have allowed the examination of fast-folding events that occur in microseconds or less, and have tested the predictions of the theoretical models.

Addresses: [1]School of Chemical Sciences, University of Illinois, Urbana, IL 61801, USA and [2]Department of Physics, University of California, San Diego, La Jolla, CA 92093, USA.

Chemistry & Biology June 1996, **3**:425–432

Introduction

For those who appreciate the beauty of the architecture of folded proteins it is amazing to find that such complex structures can be formed spontaneously in biologically short times, although doing so is clearly an evolutionary necessity. In human affairs, complex organized structures have always been made by a series of individually simple steps. A similar picture of the folding process seemed to emerge from the classical kinetic studies of folding on time scales greater than a few milliseconds [1]. But it was realized that, particularly for smaller proteins, folding could occur far more rapidly and without a requirement for this discrete stepwise assembly. This led to a view of protein folding based on a statistical mechanical characterization of the energy landscape of a folding protein ([2] and references therein), and this viewpoint has received considerable support from computational studies of model proteins [3–8]. With this new perspective it becomes clear that we will only be able to directly unravel the basic mechanisms of biomolecular self-organization and measure the topography of the folding-energy landscape with a new generation of experiments using relatively newer techniques that are capable of monitoring protein folding on shorter time scales (lasers [9–13], NMR [14–19], ultrafast mixing [20] and protein engineering [21,22]). This review highlights a remarkable fast folding experiment described in this issue by Mines *et al.* [23], who show experimentally a regularity in the folding of two proteins that is expected from a statistical description based on the landscape theory. We first discuss the theoretical descriptions of rapid protein folding before exploring to what extent the experiments of Mines *et al.*, and the increasing number of other recent fast folding experiments, support this description. Finally, we consider what the two fields have taught us so far about folding and the energy landscape.

The folding funnel

The energy-landscape theory of folding starts with the view that folding kinetics are best considered as a progressive organization of an ensemble of partially folded structures (Fig. 1), rather than a serial progression between intermediates. Thus, to understand kinetics one must statistically characterize the number and the distribution of free energies of the members of an ensemble of protein molecules that have partial order. A few collective reaction coordinates or order parameters should suffice to organize the description of the energy landscape. In contrast to most organic chemistry reactions, where the reaction coordinates describe a single structure, here they are collective coordinates characterizing an ensemble of structures as in electron transfer [24,25]. The search through these very large

Figure 1

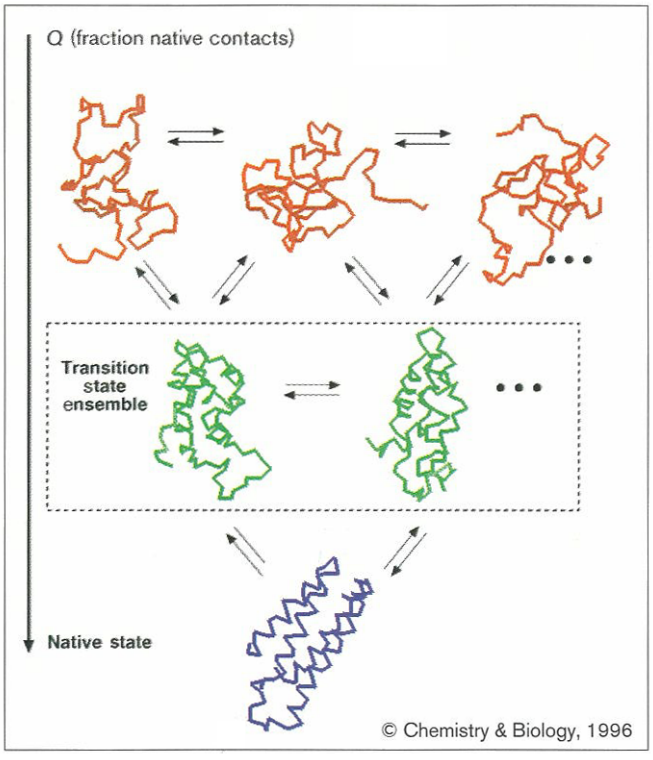

Network of conformational changes occurring in the ensemble of conformations for a protein as it folds to the native structure. The folding reaction coordinate Q is the average fraction of native contacts in members of the corresponding ensembles. The conformations in the transition state ensemble have a Q-value of ~0.6. The intermediate structures are obtained from computer simulations of a four helix bundle with varying degrees of native character. By organizing the states by energy and Q instead of the specific intermediates, a funnel description of the folding process shown in Figure 2 is obtained. (The simulations shown here are based on associative memory Hamiltonian structure prediction algorithms and show diminished helicity at low Q.)

number of configurations may present difficulties as pointed out by Levinthal years ago [26,27]. Even the protein conformations with given amounts of partial order have various energies that must be described by a distribution [28]. This give rise to what is called a 'rugged energy landscape', because many non-native interactions can exist in a (partially) disordered protein structure and these can be either favorable or non-favorable energetically. Conformational transitions from the deeper energy states in an ensemble must typically surmount an energy barrier determined both by this energetic ruggedness, ΔE^2, and any barriers provided by stereochemical constraints inherent in the polypeptide backbone.

The ruggedness of the landscape is reflected in the kinetics of escape from transient conformational traps. Fast folding would be impossible on an entirely rugged landscape, which is called a completely frustrated landscape. Fast folding is only possible because of guiding forces that stabilize correct (native) interactions, on average, more than one expects by chance. We thus say that fast-folding proteins satisfy the principle of minimal frustration [28]. On a global level, the landscape must resemble a funnel ([29–31] and J.N.O., P.G.W., Z.L.-S. & N.D. Socci, unpublished data) (Fig. 2). As a folding reaction coordinate approaches its native value, the peak in energy distribution of the ensemble of conformations shifts to a lower value, as shown in Figure 3. The mean energy of structures in the funnel goes down as the ensemble approaches the native state. Simultaneously the number of conformations decreases, reflecting a loss of configurational entropy. (The entropy of the solvent, so important for the hydrophobic force, is included in the solvent average (free) energies used in the statistical distributions characterizing the landscape.) The

Figure 2

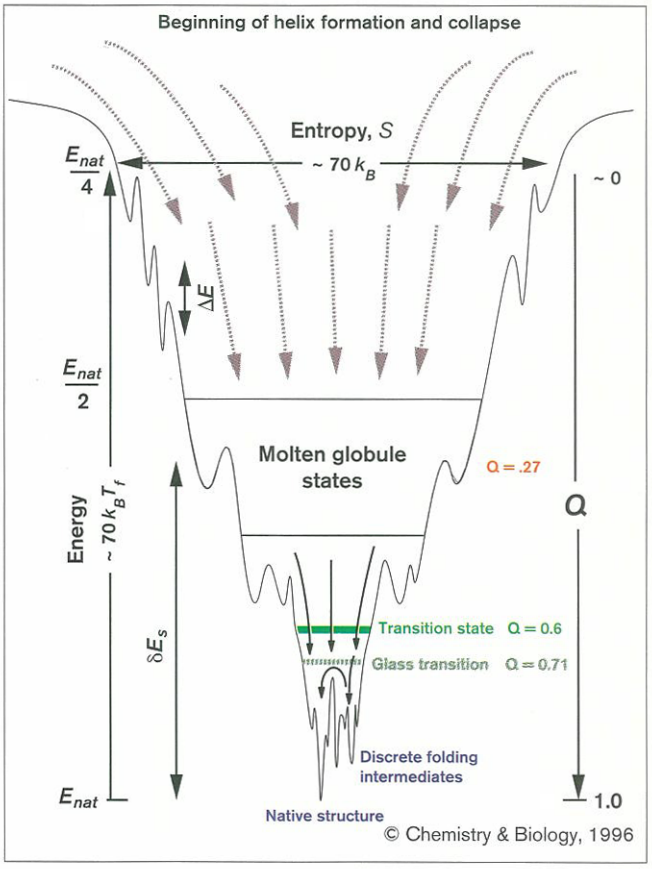

The schematic funnel for a 60-amino-acid helical protein as obtained from the corresponding-states principle analysis [30] with the 27-mer lattice model. The positions of the molten globule states, the transition state ensemble, and the local glass transition (the point at which discrete trapping states emerge) are shown as a function of the order parameters: fraction of native contacts Q, the solvents averaged energy E, and the configurational entropy S, which are drawn to scale. The stability gap δE_s quantitates the specificity of the native contacts. The ruggedness of the landscape ΔE determines the local barriers, but its value is not the conformational diffusion activation height, which is $E_a \sim 7k_BT_f$. k_B is the Boltzmann constant, T_f is the folding temperature, and E_{nat} is the energy of the native structure.

Figure 3

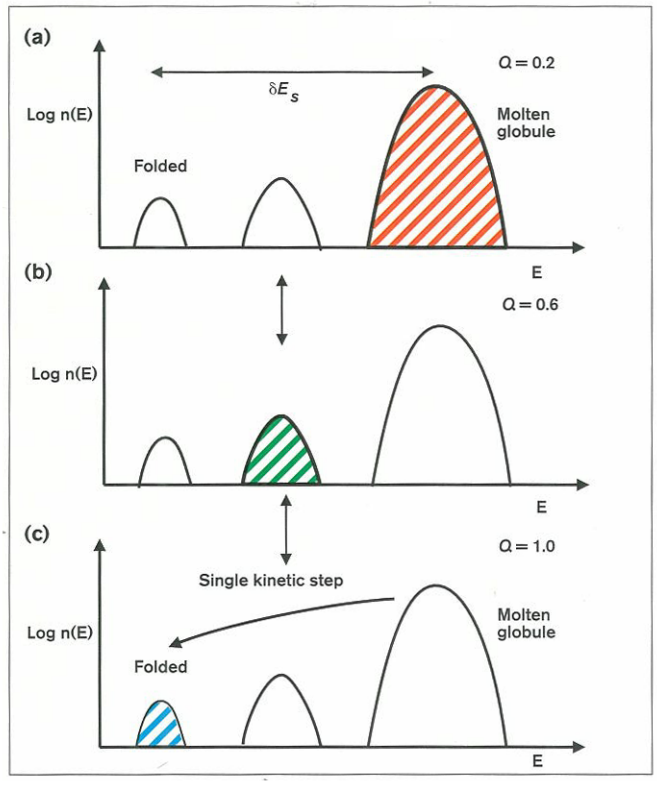

Histograms of protein configurational states at various stages of folding. **(a)** Collapsed phase with $Q = 0.2$. **(b)** Transition state with $Q = 0.6$ near the middle of the funnel. **(c)** Native state with $Q = 1.0$. In any given folding event, the protein molecule passes through intermediate Q states. In a type I folding, however, no significant population is trapped in these states, which are never substantially occupied kinetically. For downhill folding on fast time scales, these intermediate states may be sufficiently populated to be observed directly in the new fast-folding experiments. The y-axis is the logarithm of the number of configurations, and the x-axis is the free energy of a particular configuration averaged over the solvent.

mean energy loss down the funnel gives an additional energy parameter characterizing the landscape topography, the stability gap δE_s. The configurational entropy loss, the third significant parameter, is called the Levinthal entropy (S_L) as it is simply a logarithmic measure of the vastness of the configuration space of the biomolecule [30,32]. The fact that the landscape can be described by these very few parameters (δE_s, S_L, and ΔE) allows us to use a law of corresponding states (which uses scaling of certain known parameters to directly compare two different proteins) to understand the important characteristics of the funnel landscape for real proteins by investigating analytical models and lattice simulations [30]. This correspondence, and the quantitative one-dimensional funnel picture shown in Figure 2, are particularly easy to set up when collapse and non-specific secondary structure formation precede the rate-limiting stages of folding. A multidimensional funnel picture that includes additional energy scales for other collective reaction coordinates such as degree of collapse and local secondary structure has been recently developed (Z.L.-S., B.E. Ramirez & P.G.W., unpublished data) (Fig. 4). In this multidimensional picture the basic scenarios for folding remain the same, although new characteristic energies such as entropy diminution and energy loss upon collapse are needed to set up the correspondence. Fast folding experiments will allow the characterization of these important parameters, which determine a major part of the entropy loss, ultimately leading to folding.

The dominant dependence of folding on the stability gap (the difference in stability between folded and unfolded states) is strongly supported by the experiments of Gray, Winkler and colleagues [12,23]. Global changes to the

Figure 4

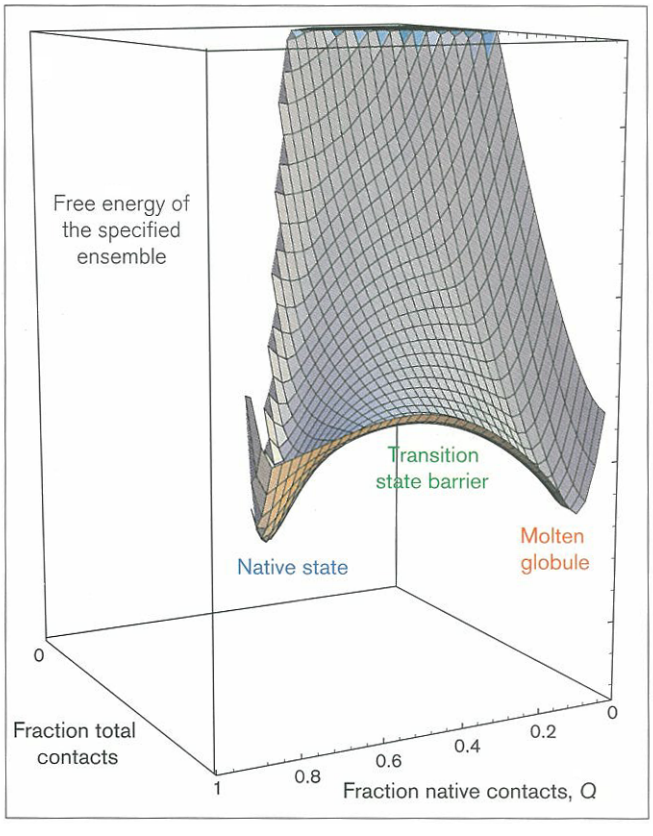

The multidimensional aspect of the free-energy surface. The average free energy of the ensemble (as opposed to that of an individual structure as shown in Fig. 2) is shown here as a function of the fraction of native contacts, Q, and total contacts. The free energies include the configurational entropy counting the number of states with a particular value of the collective coordinates. The surface is plotted using the analytical fit of Plotkin *et al.* [38], but the specific landmark values of Q are taken from the simulation results. At T_f we see two distinct minimal free energy ensembles: one (red) specifying the molten globule, the other (blue) specifying folded native-like configurations. The same transition-state ensemble (green) as in Figure 1 is represented in this lower dimensional view. The height of the thermodynamic barrier is approximately $2k_BT_f \approx 1.2$ kcal mol^{-1}.

molecule such as extensive sequence and solvent changes that lead to the same stability give a similar shaped funnel. If the corresponding-states approach were not valid, simulations of minimalist models could only be used as suggestive analogies to laboratory protein folding. Thus, this experiment encourages the application of landscape theory and simulations as quantitative tools.

Depending on the quantitative variation of entropy, mean energy and ruggedness as the protein ensemble descends in the funnel, energy-landscape theory provides a classification of kinetic scenarios [2]. If the energy loss always exceeds the entropy, we have a type 0 or 'downhill' folding scenario. Downhill folding on a relatively smooth landscape would resemble the physical process of polymer collapse and would not be expected to follow the simple exponential kinetics of a first order chemical reaction. For rougher landscapes, downhill processes would have an even wider distribution of time scales because of the varying depths of traps. These signatures should be quite obvious in fast folding experiments. For the roughest landscapes, only a few discrete traps could be populated and the dynamics could be described by a discrete but complex kinetic scheme, after the resolution of the early events. A different result is seen when the rate of energy loss down the funnel does not match, at each stage, the entropy loss as the ensemble descends. As the free energy is defined as E – TS, a free energy maximum will result when the entropy decreases more rapidly than the energy. In this type I scenario, a bottleneck occurs in the folding process. The ensemble of structures at the bottleneck represents a free energy barrier, and at the macroscopic level the folding can be described using single-step, exponential kinetics. Landscape theory predicts simple regularities for the folding-rate coefficient when the type I scenario applies. As a large number of different configurations are present at the bottleneck, detailed energetic effects on single configurations get averaged out, and thus the folding rate is largely and smoothly related to the stability.

Transfer coefficients (Φ) in local linear free energy relations (LFER) reflect the location of the bottleneck ensemble along the reaction coordinate. Using the assumption that bottleneck position does not change much when the landscape is changed, we can derive an LFER between the folding time, τ_f, and the free-energy change in folding, which to the same order is $< \Delta H >_u - < \Delta H >_f$ (J.N.O., P.G.W., Z.L.-S. & N.D. Socci, unpublished data), where the brackets indicate averaging over an ensemble. Thus:

$$\frac{\partial \log \tau_f}{\partial \log K} = \Phi = \frac{< \Delta H >_{Q^\dagger} - < \Delta H >_u}{< \Delta H >_u - < \Delta H >_f}$$

where K is the equilibrium constant for the folding reaction and the subscripts u, f and $Q^\dagger$ indicate the unfolded, folded and transition-state ensembles, respectively. F global perturbations, Φ gives a good first approximation the position of this bottleneck. Φ will be strongly cor lated to the degree of nativeness of the transition-st ensemble. Only an average description is obtain however, using a single value of Φ. Proteins are polyme leading to varying participation of different residues in t transition-state ensemble, and protein engineering tec niques reveal a histogram of participation of residues the configurations of a transition state ensemble, center around a fractional value ([21] and J.N.O., P.G.W., Z.L.- & N.D. Socci, unpublished data). Of course, as increas stabilization can transform a type I scenario to a downh one, some curvature of the LFER is also to be expected.

Type II scenarios occur if the ruggedness of the landsca is very large, so that only a few discrete trap configuratio can be thermally occupied, even before the bottleneck kinetically surmounted (type IIB). This transition to d crete long-lived traps in the type IIB scenario has much common with the glass transition, where disordered conf urations of a liquid can exist for long periods of tim Although the rough location of transition to this regime c be inferred from simple statistical mechanical theori involving the interplay of ruggedness and entropy, t most important result of landscape theory for the kinetic is the prediction that the existence of each specific trap very sensitive to even single-site changes in the molecu and might be eliminated by simple protein engineering sometimes, by chemistry [17,33]. Many of the classica studied folding processes encountered type II scenari either after a downhill run or after encountering an esp cially small entropic barrier at the bottleneck ensemb Landscape theory for type II folding can only be test quantitatively with combinatorial experiments testing t distribution of intermediate lifetimes using a variety of d ferent sequences. The fast folding events, on the oth hand, should conform to type 0 or type I scenarios a therefore will exhibit greater regularities and be dominat by the guiding forces for folding rather than ruggedne and trapping.

Fast folding experiments to date

To initiate fast folding, the protein in question mu somehow be converted, almost instantaneously, from form that favors the unfolded state to a form that fav the folded state. Several methods have recently be developed to trigger this event. The first protein to explicitly studied on the fast (submillisecond) time sc was cytochrome *c*, in an effort led by Eaton and Roc [9]. Previously, a burst phase of rapid apparent foldi had been observed in stopped flow, in which signatu of native structure were seen within the dead-time of t apparatus [17]. It was also shown that the slow phases folding were largely eliminated under pH conditic where a specific histidine is protonated and thus unal

to misassociate with the heme iron, leading to a kinetic trap [33]. Jones *et al.* [9] initiated folding photochemically by exploiting the fact that the stability of the protein is enhanced by coordination with two sidechains of the polypeptide chain. Cytochrome *c* with bound carbon monoxide thus denatures more readily than the protein that lacks CO, and flash photolysis of the CO-bound form with a laser can initiate folding within picoseconds under appropriate denaturing conditions. The change in stability is modest, so the experiment must be performed with a relatively high denaturant concentration to ensure that the initial CO-bound form is completely denatured. This procedure leads to type I folding in about 10 ms. Significantly, Jones *et al.* also observe complex spectral changes, beginning in the microsecond range. These relaxation events occur exclusively in the unfolded phase, but unfortunately all the free energy gradient in this case is caused by the differing chemical stability of the amino acids in the chain that can act as ligands of the heme and not by the dominant folding forces. Nevertheless combining these measurements of the dynamics in the unfolded state with a separate determination of the inherent chemical effects on ligand association has led to a plausible upper limit on the speed of downhill protein folding of 1 μs [34].

Gray and colleagues [12,23] exploit a conceptually similar route to fast folding. Reduced and oxidized cytochromes have different stabilities, and at a particular concentration of denaturant, the oxidized protein is unfolded and the reduced protein is folded. Thus photo-initiated electron transfer can induce folding. The oxidized, unfolded protein is bombarded with electrons, and upon conversion to the reduced form, folding is instantly favored. Using a photosensitizer electron injection system, they were able to initiate folding in less than 1 μs [12]. As the reduced cytochrome *c* in this case had a lifetime of only ~1 ms, a different injection system was used to study longer periods of time. Although it causes a larger stability change than CO binding, the electron transfer initiated folding was still studied under type I scenario conditions, giving results consistent with the earlier work, while reducing some technical difficulties arising from back reactions.

The experiment described in this issue by Mines *et al.* [23] also uses electron-transfer triggering to show a remarkable regularity that is expected for type I transitions. The part of the folding funnel probed in a type I scenario is predicted to be self-averaging, so two quite different sequences folding to the same structure should have funnel shapes in the region of high density of states (above the transition states) that depend mostly on the overall stability and amino-acid composition of the molecule. The experiments of Mines *et al.* show that horse and yeast cytochrome *c* have the same folding rates when tuned to the same stability by adjusting the denaturant concentration. This is true even though the sequences are only 50 % identical. This non-sequence-specificity of type I funnel-like folding contrasts greatly with the dynamics of type II folding; for example, the late-stage folding intermediates of lactalbumin and hen lysozyme are quite different [18]. This is true despite the fact that the two proteins share 36 % sequence identity.

Figure 5

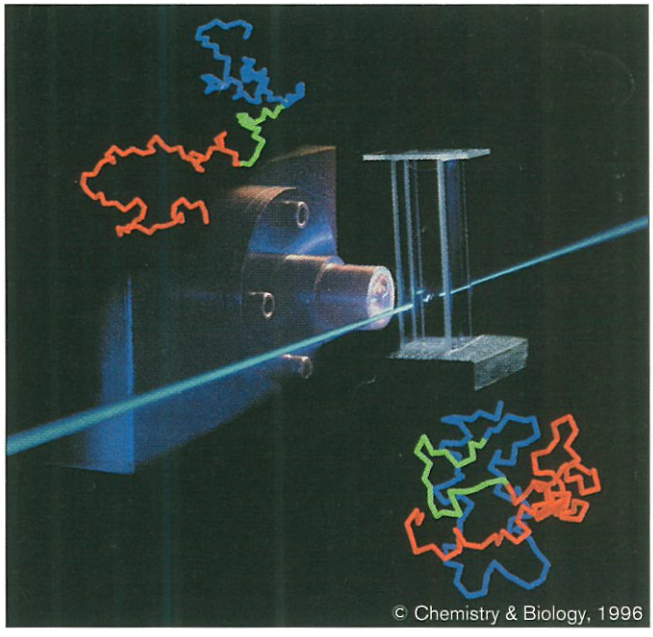

A composite picture is shown of the sample cell and laser T-jump apparatus of Ballew *et al.* [13] that was used to measure the folding of apomyoglobin from its cold-denatured state and the computer simulations of two conformations with a low (top) and high (bottom) fraction of native contacts. The conformations were obtained from a protein structure prediction simulation using an associative memory energy function [39] and are color-coded to indicate the foldon regions [35] that could be kinetically competent quasi-independent folding units.

Laser fast folding experiments can examine the dynamics of a larger portion of the folding events only by obtaining bigger stability changes. This can be achieved with a T-jump. The record for initiating folding thus far has been achieved in groundbreaking experiments of Gruebele and colleagues [13], schematically presented in Figure 5. Laser heating using an infrared pulse allows a protein that is denatured because of the cold to be taken to conditions that favor the native form within nanoseconds.

This technique to has been applied to the study of apomyoglobin, which is denatured by cold at a convenient temperature near the freezing point of water. Conformational changes can then be monitored by measuring fluorescence decay of the tryptophan by repetitive femtosecond pulses after initiating folding. Modeling the fluorescence decays at equilibrium leads to the conclusion that

the change that is detected between native and non-native states is primarily determined by a specific contact between a methionine and the tryptophan. Thus the experiment measures part of the tertiary structural transition. The data can be fit by a largely exponential process, indicating a type I scenario for this conformational change, which occurs in 7 μs. There are also some signs of shorter time scale changes in the decay, which may be connected with secondary structure formation or more local collapse of the polypeptide chain. The assignment of the major spectral change to a large-scale conformational movement is suggested by its viscosity dependence, as shown by adding glycerol to the solution. This study confirms a Kramers-like dependence of the rate on external viscosity [31]. Longer time scale measurements show that the transition seen by Gruebele and coworkers is not complete folding [19]. At least in sperm whale apomyoglobin, the complete folding occurs later. This may suggest the presence of a subdomain structure in the apomyoglobin molecule or specific traps during folding [35].

The observations of interesting dynamics on the microsecond timescale with cytochrome *c* and apomyoglobin are also confirmed in a fast T-jump experiment on barstar (barnase inhibitor) [36]. A rapid transition taking 300 μs is followed by a 100-ms slow phase. The rapid change involves a very small amplitude of fluorescence change but is clearly not an artifact. As in the experiments with cytochrome *c* [23], the location of the transition state (Φ) for this folding is early along the folding reaction coordinate as judged by its denaturant dependence. Clearly many interesting folding processes occur on the microsecond to millisecond timescale. These processes can also be observed using an enhancement of the conventional mixing techniques using small orifices. One such ultrafast mixing experiment with cytochrome *c* shows a folding process that is strongly extended and nonexponential, suggesting the possibility of a downhill or type 0 folding scenario [20]. This novel technique is still in its early stages and several complexities concerning the interaction of the turbulent hydrodynamic flows and the polymer conformations need to be sorted out in order to be completely confident of the results. Notice here that there is an apparent change of the Φ values, suggesting that nonlinearity of the free energy relation can be observed when experiments are done over a large enough range of denaturant concentrations.

NMR spectral line shape analysis can be used, at least near the midpoint of the folding curve, to study submillisecond folding dynamics. This technique has been used to examine both folding and unfolding of monomeric λ repressor [14]. This molecule is highly helical and closely resembles many of the systems studied by the theoreticians. Again an intermediate Φ value is observed showing the existence of a bottleneck or a transition state ensemble in a type I scenario near to the location predicted from theory.

Although most of the action in fast folding seems to occur in the range of microseconds, very fast processes have also been observed in unfolding experiments, such as those examining the thermally induced unfolding of apomyoglobin [11]. Protein conformation is probed using vibrational spectroscopy techniques that are sensitive to secondary structural changes. Interestingly, if the process is two-state, one of the fast unfolding processes observed could be interpreted to give a refolding time constant close to that determined by laser heating, if the temperature dependence of viscosity is taken into account. Transient infrared spectroscopy has also been used by monitor events occurring in nanosecond timescales [10]. These experiments show fairly complicated kinetics that cannot be fit by a single-step representation. Some changes occur on such short timescales that they may be accessible to direct molecular dynamics simulation [37]. Clearly a rich variety of phenomenology is beginning to appear from the submillisecond folding experiments. While many interpretational questions remain to be answered, it is quite clear that events that were earlier postulated based only on slow stopped-flow mixing experiments were just a small part of what is going on.

Quantifying funnel shapes with fast-folding experiments

We are just beginning to understand protein folding quantitatively in terms of energy-landscape topography. The fast-folding experiments we have just discussed support the qualitative notions of the theory and begin to allow us to refine the quantitative aspects of the funnel shape. Foremost among the issues in funnel shape are the questions of the appropriate coordinates for describing the crucial, partially folded ensembles of structures. In the simplest model, the fraction of native contacts (Q) is used. Because each experiment has so far used only a small fraction of the possible probes, this very basic issue still requires much study. Clearly the important configurations, as revealed in these experiments, are partially collapsed and probably have some secondary structure formed, and even though parts of the secondary structure may be in the correct locations, only a small amount of tertiary ordering may exist. Many of the next generation of experiments will begin to address these issues more completely using other techniques. Circular dichroism would be a more convincing measure of overall secondary structure, while isotopic labeling and vibrational spectroscopy could locate the precise secondary structural elements [11].

More refined fluorescence experiments using mutants with tryptophan residues placed in varying locations could pinpoint tertiary contacts. Even without the precise definition of the relevant coordinates, some quantitative features — the entropic aspects of the landscape and the ruggedness — are grossly revealed by the experiments to date and seem to have a reasonable relationship to the theoretical expectations. The fast folding experiments all suggest that

the bottleneck for folding at the midpoint of the denaturing curve corresponds to a transition state ensemble with a considerable configurational entropy. The fractional degree of folding as determined from linear free-energy relationships agrees reasonably well with results obtained from lattice simulations as expected from the corresponding states principle interpretation of the funnel landscape. This is probably the best current measure of the entropic effects in the funnel. More detailed studies of the specific contacts formed in the transition state ensemble are also in agreement with the picture that a collection of delocalized folding nuclei are important.

The ruggedness of the landscape can be quantified more accurately using the temperature dependence of the folding rate when under type I conditions or by the detailed time course in a type 0 downhill folding scenario. The data from the cytochrome *c* experiments show that configurational diffusion is faster at high temperatures than at low, as the isostability values of the folding rate are higher at 40 °C than at 22.5 °C [12,23]. Some of this effect can be attributed to the change in viscosity with temperature, as would be expected from the experiments with apomyoglobin [13], but this would only account for a small fraction of the effect. The ratios of the viscosity at these two temperatures is ~1.5, but the rate ratio is ~20. We are only able to calculate a value for the apparent activation barrier by assuming that the entire ruggedness is enthalpic (whereas it is doubtless partially entropic due to the hydrophobic effects); nevertheless, with this imperfect description we arrive at a value of $E_a \sim 11k_BT_f$. We should be very careful when providing an interpretation of such an apparent barrier [27,31]. The simplest description, using the configurational diffusion model of Bryngelson and Wolynes [27], directly relates this barrier to the average roughness of the landscape. According to their model, at temperatures sufficiently high compared to the glass transition temperature, $E_a \sim \Delta E^2/2k_BT_f \approx 10k_BT_f$. Below the glass transition temperature, the system becomes caught in a few long-lived non-native states, making the average ruggedness description invalid. The experimental value obtained for this apparent barrier is slightly larger than the actual simulated value, $E_a \sim 7k_BT_f$, using the corresponding-state analysis for a 60 residue protein. Estimates of the ruggedness and conformational diffusion activation barriers can be refined by much more extensive studies in a larger temperature and viscosity range, both for the data of Mines *et al.* [23] with a type I scenario, and the more detailed time course of an apparently type 0 scenario observed in the ultrafast mixing experiment [20].

Another fact that emerges from the fast folding experiments is that there are important fast-folding substructures in the larger proteins. In any event, the simple one-parameter funnel picture that we have highlighted in the early part of this review should apply for the smaller protein systems. The experiments with apomyoglobin suggest that a unit consisting of the A, G and H helices forms first. This unit is similar to the size of proteins described by a single funnel but clearly the overall folding may require a funnel for each substructure. A theoretical description of folding in domains or foldons has already been made using energy-landscape analysis [35].

Fast folding experiments provide the most direct view on the forces that govern the self-organization of protein molecules. The quantification of energy-landscape topography that these experiments will make possible should help structure prediction schemes that are already based on landscape ideas, but which have been handicapped by only knowing the final folded structures of proteins. Thus, we can look forward to a very fruitful interaction between the experimental community and the computational community.

Acknowledgements

The work at the University of California at San Diego was supported by the NSF (Grant No. MCB-93-16186) and at Illinois by the NIH (Grant No. 2 R01 GM44557).

References

1. Kim, P.S. & Baldwin, R.L. (1990). Intermediates in the folding reactions of small proteins. *Annu. Rev. Biochem.* **59**, 631–660.
2. Bryngelson, J.D., Onuchic, J.N., Socci, N.D., & Wolynes, P.G. (1995). Funnels, pathways and the energy landscape of protein folding: a synthesis. *Proteins* **21**, 167–195.
3. Friedrichs, M. & Wolynes, P.G. (1990). Molecular dynamics of associative memory Hamiltonians for protein tertiary structure recognition. *Tetrahedron (Comp. Meth)* **3**, 175–190.
4. Dill, K.A., *et al.*, & Chan, H.S. (1995). Principles of protein folding: a perspective from simple exact models. *Protein Sci.* **4**, 561–602.
5. Honeycutt, J.D. & Thirumalai, D. (1992). The nature of the folded state of globular proteins. *Biopolymers* **32**, 695–709.
6. Sali, A., Shakhnovich, E. & Karplus, M. (1994). Kinetics of protein folding: a lattice model study of the requirements for folding to the native state. *J. Mol. Biol.* **235**, 1614–1636.
7. Socci, N.D. & Onuchic, J.N. (1994). Folding kinetics of protein-like heteropolymers. *J. Chem. Phys.* **101**, 1519–1528.
8. Socci, N.D. & Onuchic, J.N. (1995). Kinetic and thermodynamic analysis of protein-like heteropolymers: Monte Carlo histogram technique. *J. Chem. Phys.* **103**, 4732–4744.
9. Jones, C.M., *et al.*, & Eaton, W.A. (1993). Fast events in protein folding initiated by nanosecond laser photolysis. *Proc. Natl. Acad. Sci. USA* **90**, 11860–11864.
10. Phillips, C.M., Mizutani, Y. & Hochstrasser, R.M. (1995). Ultrafast thermally induced unfolding of RNase A. *Proc. Natl. Acad. Sci. USA* **92**, 7292–7296.
11. Williams, S., *et al.*, & Dyer, R.B. (1996). Fast events in protein folding, helix melting and formation in a small peptide. *Biochemistry* **36**, 691–698.
12. Pascher, T., Chesick, J.P., Winkler, J.R. & Gray, H.B. (1996). Protein folding triggered by electron transfer. *Science* **271**, 1558–1560.
13. Ballew, R.M., Sabelko, J. & Gruebele, M. (1996). Direct observation of fast protein folding: the initial collapse of apomyoglobin. *Proc. Natl. Acad. USA* **93**, 5759–5764.
14. Huang, G.S. & Oas, T.G. (1995). Submillisecond folding of monomeric λ repressor. *Proc. Natl. Acad. Sci. USA* **92**, 6878–6882.
15. Feng, Y., Sligar, S.G. & Wand, A.J. (1994). The solution structure of apocytochrome b_{562}. *Nat. Struct. Biol.* **1**, 30–36.
16. Nash, D., Lee, B. & Jonas, J. (1996). Hydrogen exchange kinetics in the cold denatured state of ribonuclease A. *Biochim. Biophys. Acta*, in press.
17. Roder, H. & Elove, G.A. (1994). Early stages of protein folding. In

Mechanisms of Protein Folding. (Pain, R.H., ed.), pp. 26–54, Oxford Press, Oxford.
18. Alexandrescu, A.T., Evans, P.A., Pitkeathly, M., Baum, J. & Dobson, C.M. (1993). Structure and dynamics of the acid-denatured molten globule state of α-lactalbumin: a two-dimensional NMR study. *Biochemistry* **32**, 1707–1718.
19. Wright, P.E. & Jennings, P.A. (1993). Formation of a molten globule intermediate early in the kinetic folding pathway of apomyoglobin. *Science* **262**, 892–895.
20. Chan, C-K., Hu, Y., Takahashi, S., Rousseau, D.L., Eaton, W.A. & Hofrichter, J. (1996). Protein folding kinetics studied by ultrafast mixing. *Biophys. J.* **70**, A177.
21. Itzhaki, L.S., Otzen, D.E. & Fersht, A.R. (1995). The structure of the transition state for folding of chymotrypsin inhibitor 2 analysed by protein engineering methods: evidence for a nucleation-condensation mechanism for protein folding. *J. Mol. Biol.* **254**, 260–288.
22. López-Hernández, E. & Serrano, L. (1996). Structure of the transition state for folding of the 129 amino acid protein CheY resembles that of a smaller protein, CI-2. *Fold. Des.* **1**, 43–55.
23. Mines, G.A., Pascher, T., Lee, S.C., Winkler, J.R. & Gray, H.B. (1996). Cytochrome *c* folding triggered by electron transfer. *Chemistry & Biology* **3**, 491–497.
24. Onuchic, J.N. & Wolynes, P.G. (1993). Energy landscapes, glass transitions and chemical reaction dynamics in biomolecular or solvent environment. *J. Chem. Phys.* **98**, 2218–2224.
25. Marcus, R.A. (1993). Electron transfer reactions in chemistry: theory and experiment. *Rev. Mod. Phys.* **65**, 599–610.
26. Levinthal, C. (1969). How to fold graciously. In *Mossbauer Spectroscopy in Biological Systems.* (DeBrunner, P., Tsibris, J. & Munck, E., eds), pp. 22–24, University of Illinois Press, Urbana, IL.
27. Bryngelson, J.D. & Wolynes, P.G. (1989). Intermediates and barrier crossing in a random energy model (with applications to protein folding). *J. Phys. Chem.* **93**, 6902–6915.
28. Bryngelson, J.D. & Wolynes, P.G. (1987). Spin glasses and the statistical mechanics of protein folding. *Proc. Natl. Acad. Sci. USA* **84**, 7524–7528.
29. Leopold, P.E., Montal, M. & Onuchic, J.N. (1992). Protein folding funnels: a kinetic approach to the sequence–structure relationship. *Proc. Natl. Acad. USA* **89**, 8721–8725.
30. Onuchic, J.N., Wolynes, P.G., Luthey-Schulten, Z. & Socci, N.D. (1995). Towards an outline of the topography of a realistic protein folding funnel. *Proc. Natl. Acad. Sci. USA* **92**, 3626–3630.
31. Socci, N.D., Onuchic, J.N. & Wolynes, P.G. (1996). Diffusive dynamics of the reaction coordinate for protein folding funnels. *J. Chem. Phys.* **104**, 5860–5868.
32. Luthey-Schulten, Z.A., Ramirez, B.E. & Wolynes, P.G. (1995). Helix–coil, liquid–crystal and spin–glass transitions of a collapsed heteropolymer. *J. Phys. Chem.* **99**, 2177–2185.
33. Sosnick, T.R., Mayne, L., Hiller, R. & Englander, S.W. (1994). The barriers in protein folding. *Nat. Struct. Biol.* **1**, 149–156.
34. Hagen, S.J., Hofrichter, J., Szabo, A. & Eaton, W.A. (1996). Diffusion limited contact formation in unfolded cytochrome *c:* estimating the maximum rate of protein folding. *Proc. Natl. Acad. Sci.*, in press.
35. Panchenko, A.R., Luthey-Schulten, Z.A. & Wolynes, P.G. (1996). Foldons, protein structural modules and exons. *Proc. Natl. Acad. Sci. USA* **93**, 2008–2013.
36. Nolting, B., Golbik, R. & Fersht, A.R. (1995). Submillisecond events in protein folding. *Proc. Natl. Acad. Sci. USA* **92**, 10668–10672.
37. Daggett, V. & Levitt, M. (1992). A model of the molten globule state from molecular dynamics simulations. *Proc. Natl. Acad. Sci. USA* **89**, 5142–5146.
38. Plotkin, S.S., Wang, J. & Wolynes, P.G. (1996). A correlated energy landscape model for finite, random heteropolymers. *Phys. Rev. E*, in press.
39. Goldstein, R.A. Luthey-Schulten, Z.A. & Wolynes, P.G. (1992). Optimal protein-folding codes from spin-glass theory. *Proc. Natl. Acad. Sci. USA* **89**, 4918–4922.